Catalysis Science & Technology

PAPER

View Article Online
View Journal | View Issue

Cite this: *Catal. Sci. Technol.*, 2014, 4, 4433

Towards highly selective ethylene epoxidation catalysts using hydrogen peroxide and tungsten- or niobium-incorporated mesoporous silicate (KIT-6)†

Wenjuan Yan,[ab] Anand Ramanathan,[a] Madhav Ghanta‡[ab] and Bala Subramaniam*[ab]

Received 6th July 2014,
Accepted 2nd August 2014

DOI: 10.1039/c4cy00877d

www.rsc.org/catalysis

Significant ethylene epoxidation activity was observed over Nb- and W-incorporated KIT-6 materials with aqueous hydrogen peroxide (H_2O_2) as the oxidant and methanol as solvent under mild operating conditions (35 °C and 50 bar) where CO_2 formation is avoided. The Nb-KIT-6 materials generally show greater epoxidation activity compared to the W-KIT-6 materials. Further, the ethylene oxide (EO) productivity observed with these materials [30–800 mg EO h^{-1} (g metal)$^{-1}$] is of the same order of magnitude as that of the conventional silver (Ag)-based gas phase ethylene epoxidation process. Our results reveal that the framework-incorporated metal species, rather than the extra-framework metal oxide species, are mainly responsible for the observed epoxidation activity. However, the tetrahedrally coordinated framework metal species also introduce Lewis acidity that promotes their solvolysis (which in turn results in their gradual leaching) as well as H_2O_2 decomposition. These results and mechanistic insights provide rational guidance for developing catalysts with improved leaching resistance and minimal H_2O_2 decomposition.

1. Introduction

Ethylene oxide (EO) is one of the widely used chemical intermediates, with applications in the production of detergents, thickeners, solvents, plastics and various organic chemicals. In 2013, the global EO production capacity was approximately 20.5 million metric tons. During the next decade, the EO demand is projected to grow at an annual rate of 6–7%.[1] Currently, EO is produced through vapor phase ethylene epoxidation over Ag-based catalysts using O_2 as the oxidant. A major challenge in this technology has been to curtail the burning of ethylene as well as EO to CO_2 at typical reaction temperatures (200–240 °C). To reduce burning, promoters such as Cs, Cd, Cu and Pt have been added to the Ag catalyst.[2–4] Such catalyst modifications have resulted in remarkable enhancements in EO selectivity, from 45% in 1945 to approximately 90% at present. Despite these improvements, the CO_2 released as a by-product is still approximately 3.4 million metric tons per year, making it the second largest emitter of CO_2 among all chemical processes after ammonia synthesis. Further, ethylene burning alone translates to a monetary loss of approximately $1.6 billion per year assuming an ethylene price of 32¢ lb^{-1}.[5]

With the increased availability of ethane as a collateral product from shale gas recovery, alternate EO technologies that better conserve ethylene feedstock have assumed renewed importance. Recently, we reported a liquid phase ethylene epoxidation process (also referred herein as the CEBC process) that eliminates ethylene burning and produces EO with nearly total selectivity.[1,6,7] Under mild operating conditions of 40 °C and 50 bar, the catalyst (methyltrioxorhenium, MTO) shows high activity (1610–4970 mg EO h^{-1} (g Re)$^{-1}$) with H_2O_2 fully utilized toward EO formation.[1] The oxidant (H_2O_2), operating conditions (20–40 °C, 50 bar) and solvent (methanol) are very similar to those employed in the Dow-BASF HPPO technology for making propylene oxide.[8] The main difference is that the HPPO process uses a heterogeneous TS-1 catalyst that does not work for ethylene epoxidation. Preliminary economic analysis suggests that the Re-based EO process has the potential to be competitive if Re recycling is nearly quantitative.[7] The EO production cost *via* the conventional Ag-catalyzed process is estimated to be 58¢ lb^{-1}. The corresponding EO production cost *via* the MTO-catalyzed process is 57¢ lb^{-1}, when assuming a catalyst life of 1 year and a leaching rate of 0.11 lb MTO h^{-1}. The

[a] *Center for Environmentally Beneficial Catalysis, Lawrence, Kansas 66047, USA. E-mail: bsubramaniam@ku.edu; Fax: +1 785 864 6051; Tel: +1 785 864 2903*
[b] *Department of Chemical and Petroleum Engineering, University of Kansas, Lawrence, KS 66045, USA*

† Electronic supplementary information (ESI) available. See DOI: 10.1039/c4cy00877d

‡ Currently with SABIC Innovative Plastics, Selkirk, NY 12158, USA.

costs of the oxidant (H_2O_2) and the catalyst (Re-based) in the CEBC process are significantly higher than those of their counterparts (O_2 and Ag, respectively) in the conventional process. However, the higher oxidant and catalyst costs are offset by gains made in other operating costs stemming from more effective ethylene utilization in the CEBC process. Yet, the performance metrics (on catalyst life, activity and maximum catalyst leaching rate) for practical viability of the CEBC process are rather demanding. This aspect, coupled with low abundance and high cost of the Re metal ($1400 lb^{-1}), poses significant challenges for the commercialization of any Re-based technology and prompted us to investigate alternative ethylene epoxidation catalysts that are relatively inexpensive and heterogeneous in nature.

In this context, W- and Nb-modified heterogeneous catalysts on MCM-41- and SBA-15-type supports have been shown to exhibit excellent catalytic activities for epoxidation of cyclohexene,[9–11] cyclooctene,[9,12–14] and methyl oleate.[15,16] However, two of the important performance measures, *viz.*, the stability of H_2O_2 against decomposition and metal leaching from the catalysts, have not been clearly addressed in the literature. In the present study, we have synthesized and evaluated W (ref. 17) and Nb (ref. 18) incorporated mesoporous materials for ethylene epoxidation with H_2O_2 as the oxidant under mild conditions (35 °C and 50 bar).[19] We chose silica-based cubic mesoporous supports (KIT-6, KIT-5) that have attracted much attention in recent years due to their high surface area and uniform pore size.[20,21] In evaluating the performance of these catalysts, we investigated metal leaching and H_2O_2 stability, critical aspects to establish practical viability. The W-KIT-6 and Nb-KIT-6 catalysts are shown to be active for ethylene epoxidation under mild conditions. However, significant H_2O_2 decomposition and metal leaching from the catalyst were observed. Plausible mechanisms for both epoxidation and catalyst deactivation are proposed with a view to rationally developing improved catalysts that display near-quantitative EO selectivity while also thwarting H_2O_2 decomposition and metal leaching.

2. Experimental

2.1 Materials

Methanol (MeOH), employed as solvent, was used as received without further purification. Ceric sulfate (0.1 N) and trace metal grade sulfuric acid (99.9 wt.%) were purchased from Fisher Scientific. Ethylene (high purity grade) was purchased from Matheson Tri-Gas Co. The oxidant (50 wt% H_2O_2 in H_2O), ferroin indicator solution, acetonitrile (AN) (HPLC grade 99.9 wt.% purity), anhydrous ethylene glycol (EG), sodium tungstate, tungstic acid and tungsten(VI) oxide (WO_3) powder were purchased from Sigma-Aldrich and used without further purification. Nb_2O_5 and niobium oxalate were purchased from Strem Chemicals and used as received. The EO standard was purchased from Supelco Analytical.

2.2 Catalyst synthesis and characterization

Mesoporous W-KIT-6 and Nb-KIT-6 catalytic materials used in this study were synthesized and characterized in detail, as reported elsewhere.[17,18]

2.3 Silylation of Nb-KIT-6 using hexamethyldisilazane (HMDS)

In a typical silylation procedure, 2 g of Nb-KIT-6 (Si/Nb = 40) was heated to 120 °C under vacuum for 12 h. The calcined material was then dispersed in 30 mL of a 5 wt.% solution of HMDS in dry toluene. The dispersion was stirred for 7 h at 120 °C. The resulting solid was filtered and washed with 100 mL of dry toluene and 200 mL of anhydrous ethanol. This process was repeated thrice.

2.4 Catalytic epoxidation studies

The schematic of the reactor setup is shown in Fig. S1 (ESI†). The reactor and the operating procedure have been described previously.[1] Briefly, the catalysts were tested for ethylene epoxidation in a 50 mL Parr reactor operated at 35 °C, 50 bar and 1400 rpm (to eliminate gas–liquid mass transfer limitations). Under these conditions, ethylene (P_c = 50.6 ± 0.5 bar, T_c = 9.3 ± 0.5 °C) is near its critical point and hence exhibits liquid-like density, causing it to substantially dissolve in the liquid phase, expanding its volume by up to 15%.[1] Thus, the reaction occurs in an ethylene-expanded liquid phase. Prior to reaction, the catalyst samples were activated in a stream of flowing air at 500 °C for 5 h with a heating rate of 2 °C min^{-1}. A mixture containing 50 wt.% H_2O_2/H_2O solution (118 mmol H_2O_2), MeOH (624 mmol) and acetonitrile (AN) as the internal standard (4.9 mmol) was charged into the Parr reactor. Isothermal batch reactions lasting up to 5 h were performed at constant pressure with each catalyst sample. The reaction mixture was sampled at regular intervals to determine the concentrations of the desired product (EO) and the by-products [ethylene glycol (EG) and 2-methoxyethanol (2-ME)]. A Hewlett-Packard 5890 Series II gas chromatograph (GC) employing a CP-WAX 58 (FFAP) CB capillary column (25 m × 0.25 mm × 0.2 μm), equipped with a flame ionization detector, was used for the analysis of the liquid phase. Fig. S2 (ESI†) shows a sample chromatogram with well-resolved GC/FID peaks for ethylene, EO, MeOH, AN, 2-ME and EG. The H_2O_2 concentration in the reaction mixture, before and after reaction, was determined by redox titration with ceric(IV) sulfate and ferroin indicator. Both the fresh and the used catalysts were digested with HF and H_2SO_4 in an autoclave at 100 °C for up to 5 h, and the resulting solution was used for performing elemental analysis by ICP-OES.

The following definitions are used in assessing the performance of the tested catalysts:

$$\mathrm{TOF} = \frac{m_{\mathrm{EO}}}{(\text{batch time})(m_{\text{metal}})}$$

$$S_{EO} = \left(\frac{n_{EO}}{n_{EO} + n_{2\text{-ME}} + n_{EG}} \right) \times 100\%$$

$$U_{H_2O_2} = \frac{n_{EO} + n_{2\text{-ME}} + n_{EG}}{n_{H_2O_2}{}^{0} - n_{H_2O_2}} \times 100\%$$

$$X_{H_2O_2} = \frac{n_{H_2O_2}{}^{0} - n_{H_2O_2}}{n_{H_2O_2}{}^{0}} \times 100\%$$

where TOF, S_{EO}, $U_{H_2O_2}$, and $X_{H_2O_2}$ denote EO productivity (mg EO h^{-1} (g metal)$^{-1}$), EO selectivity, H_2O_2 utilization toward EO formation (also defined as the H_2O_2 utilization efficiency) and H_2O_2 conversion, respectively, and m_{EO} and n_{EO} represent the mass of EO formed and the mass of metal in the catalyst, respectively.

n_{EO}, $n_{2\text{-ME}}$ and n_{EG} denote the molar amounts of EO, 2-ME and EG formed, respectively.

$n_{H_2O_2}{}^{0}$ and $n_{H_2O_2}$ denote the initial and the final molar amounts of H_2O_2, respectively. As shown in Tables 2 and 4, the uncertainty in the measured values of the various performance metrics, established through repeated runs, is within 3% of the reported mean values.

3. Results and discussion

3.1 Catalyst characterization

Detailed physicochemical characterization of the catalyst samples may be found elsewhere.[17,18] Only the salient features are summarized here. The mesoporous nature of W and Nb catalyst samples was confirmed by small angle X-ray scattering and N_2 sorption. The physicochemical characteristics are summarized in Table 1. For all of the samples, the surface area ranges from 625 to 997 m^2 g^{-1}, decreasing at increased metal loadings (1.5–17.9 wt.%). In general, Nb-KIT-6 materials display larger pore diameter (8.5 nm) and lower acidity (0.11–034 mmol NH_3 g^{-1}) compared to W-KIT-6 (6.4–6.9 nm and 0.26–0.46 mmol NH_3 g^{-1}). Diffuse reflectance UV-vis characterization reveals that W is incorporated in the catalyst in at least three forms as follows: isolated tetrahedrally coordinated WO_4 (~206 nm), nanoparticles of WO_3 (~270 nm) and bulk WO_3 (~420 nm, observed only at higher W loadings).[17] In contrast, for Nb-KIT-6, only the absorption peak due to isolated framework-incorporated NbO_4 was noticed at 195 nm. Even at the highest Nb loading, no absorption bands around 320–340 nm, characteristic of Nb_2O_5 species, are evident. However, the bands at 220 and 270 nm suggest that oligomeric NbO_4 units are present in all samples even at low Nb loadings.[18]

3.2 Catalyst performance for ethylene epoxidation

3.2.1 Intrinsic activity. W-KIT-6 and Nb-KIT-6 catalysts were tested to compare EO productivity, EO selectivity, H_2O_2 utilization for EO formation and metal leaching. The results are summarized in Table 2. The support material, Si-KIT-6, showed negligible EO formation. However, under similar operating conditions, W- and Nb-incorporated KIT-6 materials are active for ethylene epoxidation. The TOF values observed with W-KIT-6 (34–152 mg EO h^{-1} (g W)$^{-1}$) and Nb-KIT-6 (234–794 mg EO h^{-1} (g Nb)$^{-1}$) catalysts are lower than those reported for conventional Ag catalysts (700–4400 mg EO h^{-1} (g Ag)$^{-1}$).[22] The initial epoxidation rate (R_{EO}) estimated from the slope of the temporal formation profile at an early time was used to quantitatively assess the significance of gas–liquid (α_1), liquid–solid (α_2) and intraparticle mass transfer resistances (ϕ), employing established criteria (Table 3).[23,24] The estimated values of α_1, α_2 and ϕ are 1.83 (10^{-4}), 3 (10^{-13}) and 9.5 (10^{-14}), respectively, indicating that both external and intraparticle mass transfer limitations are insignificant at the investigated conditions. Details of estimating these parameters are presented in Tables S1 and S2 (ESI†).

As inferred from Table 2 (entries 1–4), the TOF generally decreased with an increase in the W content. For example, the TOF decreased from 152.6 to 34.4 mg EO h^{-1} (g W)$^{-1}$ as the W loading increased from 2.2 to 17.9 wt%. A similar trend was also observed with Nb-KIT-6 catalysts (Table 2, entries 5–8). These results might suggest that the extra-framework oxide species observed at higher metal loadings may not be active for epoxidation. Indeed, significantly lower EO TOFs are observed when WO_3, H_2WO_4, Na_2WO_4 (see Table 2, entries 9, 10 and 11), Nb_2O_5 and niobium oxalate (see Table 2, entries 12 and 13) were tested under similar operating conditions.

Even though all of the tested catalysts show activity for ethylene epoxidation, H_2O_2 utilization efficiency ($U_{H_2O_2}$) ranges from 1.0 to 18.8% (Table 2) and is thus low. In the absence of ethylene, H_2O_2 conversion under otherwise

Table 1 Physicochemical characteristics of W- and Nb-KIT-6 catalysts[15,16]

Catalyst[a]	M wt%	S_{BET}[b] (m^2 g^{-1})	$V_{p,BJH}$[c] (cm^3 g^{-1})	$d_{p,BJH}$[d] (nm)	mmol NH_3 g^{-1}
W-KIT-6(10)	17.9	625	1.09	6.9	0.30
W-KIT-6(20)	9.4	778	1.23	6.7	0.33
W-KIT-6(40)	5.7	832	1.29	6.3	0.26
W-KIT-6(100)	2.2	927	1.44	6.4	0.12
Nb-KIT-6(10)	13.4	804	1.01	8.5	0.34
Nb-KIT-6(20)	7.2	926	1.16	8.5	0.23
Nb-KIT-6(40)	3.7	991	1.2	8.5	0.15
Nb-KIT-6(100)	1.5	997	1.35	8.5	0.11

[a] The number in parentheses represents the Si/M molar ratio. [b] S_{BET} = specific surface area. [c] $V_{P,BJH}$ = pore volume. [d] $d_{P,BJH}$ = pore diameter.

Table 2 Epoxidation activity of ethylene over W-KIT-6 and Nb-KIT-6 catalysts (reaction conditions: MeOH = 624 mmol, H_2O_2 = 118 mmol, AN = 4.9 mmol, catalyst loading = 500 mg, T = 35 °C, ethylene P = 50 bar (maintained constant), t = 5 h, 1400 rpm)

#	Catalyst[a]	M wt%	EO TOF (±3%)	S_{EO}% (±3%)	$X_{H_2O_2}$% (±3%)	$U_{H_2O_2}$% (±3%)
1	W-KIT-6(10)	17.9	34.4	81.4	10.2	3.6
2	W-KIT-6(20)	9.4	43.4	80.0	6.4	3.9
3	W-KIT-6(40)	5.7	66.5	84.0	6.0	3.5
4	W-KIT-6(100)	2.2	152.6	80.0	4.2	5.0
5	Nb-KIT-6(10)	13.4	234	46.8	17.1	18.8
6	Nb-KIT-6(20)	7.2	340	52.7	17.1	13.1
7	Nb-KIT-6(40)	3.7	513	62.6	17.5	8.4
8	Nb-KIT-6(100)	1.5	794	73.4	11.2	7.1
9	WO_3	79.3	2.49	91.7	2.5	3.7
10	H_2WO_4	73.6	2.63	100.0	6.4	1.3
11	Na_2WO_4	72.1	10.7	94.4	5.2	5.6
12	Nb_2O_5	69.9	4.38	89.5	4.1	4.0
13	Niobium oxalate	51.4	10.1	90.0	8.8	1.0
14	W-KIT-6(100)[b]	0.57	450	94.1	6.8	2.1
15	W-KIT-6(100)[c]	0.24	298	100.0	3.5	2.4
16	Nb-KIT-6(10)[b]	8.9	284	58.3	8.0	14.0
17	Nb-KIT-6(20)[b]	4.9	372	70.0	6.5	10.4
18	Nb-KIT-6(40)[b]	1.4	844	69.1	4.7	9.8
19	Nb-KIT-6(100)[b]	0.4	1789	59.5	4.7	6.7
20	Nb-KIT-6(40)-B2[d]	3.3	400	64.7	38.7	3.0
21	Nb-KIT-6(40)-B2[e]	2.9	328	79.4	12.8	5.3
22	Si-KIT-6[f]	0	0	0	0	0
23	Nb-KIT-6(10)[g]	13.4	0	0	14.1	0

[a] The number in the parenthesis represents the Si/M molar ratio. [b] After the 1st 5 h run. [c] After the 2nd 5 h run. [d] Fresh batch of Nb-KIT-6(40). [e] Silylated Nb-KIT-6(40)-B2. [f] Blank run with KIT-6 support as the catalyst. [g] Blank run with no ethylene in the reaction.

similar operating conditions was 14.1% (Table 2, entry 23) even on Nb-KIT-6, which shows the highest H_2O_2 utilization efficiency for EO formation (~18%). However, no detectable H_2O_2 decomposition was observed with just the support material (Si-KIT-6) during a run without substrate (ethylene) under similar operating conditions (Table 2, entry 22). This suggests that the acidity imparted by metal incorporation into the KIT-6 support (see Table 1) is a causative factor for H_2O_2 decomposition.

The effect of temperature on EO productivity was investigated with the Nb-KIT-6 catalyst that showed the highest activity (Si/Nb = 20). As inferred from Table 4, whereas increasing the temperature from 35 to 50 °C has little effect on the TOF, EO selectivity decreased significantly from 76.3 to 38.2% as side reactions begin to dominate. In addition, enhanced H_2O_2 conversion ($X_{H_2O_2}$) but lower H_2O_2 utilization efficiency ($U_{H_2O_2}$) was noticed at the higher temperatures.

Fig. 1 shows the temporal variations in the formation of EO and other liquid phase products (EG and 2-ME) over Nb-KIT-6 (Si/Nb = 20) at 35 °C. Clearly, EO selectivity decreases with time due to several parallel adverse events, including reaction of EO to form side products (such as EG and 2-ME), metal leaching and H_2O_2 decomposition. It is known that the presence of water blocks Lewis acid sites and forms Brønsted acid sites.[10] While Lewis acidity enhances ethylene conversion and stabilizes the epoxide, Brønsted acid sites are known to favor the ring opening of chemisorbed epoxide to form the glycol.[25] As shown in Fig. 2, EO selectivity decreases significantly over Nb-KIT-6 catalysts as the number of Brønsted acid sites increases.[18]

3.2.2 Catalyst/H_2O_2 stability. Recycle tests were carried out with selected catalyst samples up to two cycles. Following the initial run with the fresh catalyst, the recovered solids were calcined in air at 500 °C for 5 h and reused. As summarized in Table 5, ICP-OES analysis of the spent reaction mixture revealed that 32–75% of the metal in the catalyst had leached

Table 3 Estimates confirming the absence of mass transfer limitations[a]

Mass transfer step	Criterion	Estimated value
Gas–liquid	$\alpha_1 = \frac{R_{EO}}{k_l a C_{H_2O_2}} < 0.1$	1.83 (10^{-4})
Liquid–solid	$\alpha_2 = \frac{R_{EO}}{k_s a_p C_{H_2O_2}} < 0.1$	3 (10^{-13})
Intraparticle	$\phi_{exp} = \frac{d_p}{6}\left[\frac{(n+1)\rho_p R_{EO}}{2D_e w C_{H_2O_2}}\right]^{\frac{1}{2}} < 0.2$	9.5 (10^{-4})

[a] Details of calculations are shown in Tables S1 and S2 (ESI).

Table 4 Effect of temperature on ethylene epoxidation activity over Nb-KIT-6(20) (reaction conditions: MeOH = 624 mmol, H_2O_2 = 118 mmol, AN = 4.9 mmol, catalysts = 500 mg, ethylene P = 50 bar (maintained constant), t = 5 h, 1400 rpm)

T °C	EO TOFs (±3%)	S_{EO}% (±3%)	$X_{H_2O_2}$% (±3%)	$U_{H_2O_2}$% (±3%)
35	447	76.3	15.1	13.5
40	428	62.9	20.3	11.6
50	438	38.2	36.9	10.8

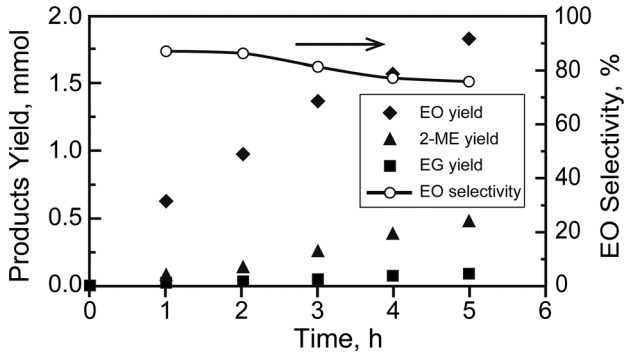

Fig. 1 Temporal variations in the formation of EO and by-products over Nb-KIT-6(20) at 35 °C.

out during the first 5 h run. Interestingly, as shown in Table 2 (entries 14–19), the TOF of the recycled W-KIT-6 and Nb-KIT-6 catalysts increased during the second 5 h run with the recovered catalysts from the first run. This suggests that inactive metal species (such as the oxides) initially leach out. However, as seen with the W-KIT-6 samples, the framework-incorporated metal species also leach out in subsequent recycles resulting in a TOF decrease during the second recycle run (Table 2, entry 15), eventually causing complete catalyst deactivation. Similar leaching was reported from heterogeneous catalysts based on Mo, W, Cr, V and Ti[26–28] in the presence of either H_2O_2 alone or H_2O_2 along with the substrate. In our experiments, we also observe substantial leaching of tungsten species during a blank experiment with only H_2O_2 and without methanol or ethylene (Table 5, entry 13). Further, we observe reduced tungsten leaching (24% in 5 h) during a blank run with only the solvent (Table 5, entry 12). In this case, we suspect that the extra-framework oxide species, rather than the framework metal species, are being primarily leached.

In addition to metal leaching, we also observe H_2O_2 decomposition on the M-KIT-6 catalysts. Interestingly, our experimental results (entries 22 and 23, Table 2) unambiguously show that H_2O_2 is stable on the KIT-6 support (with either low or no measurable acidity), suggesting that the

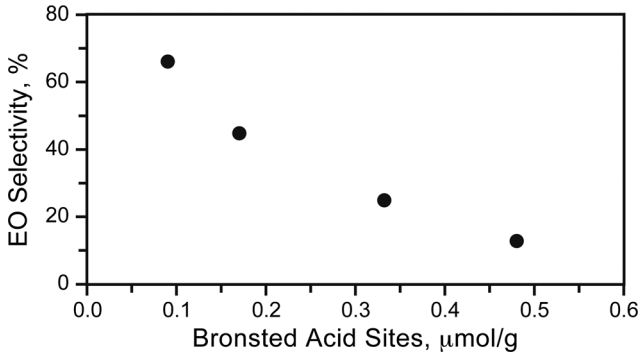

Fig. 2 Detrimental effect of Brønsted acid sites on EO selectivity over different Nb-KIT-6 catalysts (Brønsted acidity values taken from ref. 16). Experimental conditions are the same as those listed in Table 2.

Table 5 Metal leaching from W-KIT-6 and Nb-KIT-6 catalysts (reaction conditions: MeOH = 624 mmol, H_2O_2 = 118 mmol, AN = 4.9 mmol, catalyst loading = 500 mg, T = 35 °C, ethylene P = 50 bar (maintained constant), t = 5 h, 1400 rpm)

#	Catalyst[a]	Leaching ±5%
1	W-KIT-6(100)[b]	74.1
2	W-KIT-6(100)[c]	89.1
5	Nb-KIT-6(10)[b]	33.7
6	Nb-KIT-6(20)[b]	32.4
7	Nb-KIT-6(40)[b]	61.6
8	Nb-KIT-6(100)[b]	72.4
9	Nb-KIT-6(40)-B2[d,b]	36.1
10	Nb-KIT-6(40)-B2[e,b]	26.4
11	Nb-KIT-6(40)-B2[e,b,f]	9.1
12	W-KIT-6(100)[g]	24.0
13	W-KIT-6(100)[h]	100

[a] The number in parentheses represents the Si/M ratio. [b] After the 1st 5 h run. [c] After the 2nd 5 h run. [d] Calcined Nb-KIT-6(40)-B2. [e] Silylated Nb-KIT-6(40)-B2. [f] Silica leaching from the silylated catalyst. [g] Blank run of leaching experiments in the presence of methanol only (without H_2O_2 or ethylene). [h] Blank run of leaching experiments in the presence of H_2O_2 only (without methanol or ethylene).

significant acidity measured on M-KIT-6 materials causes H_2O_2 decomposition.

Based on the foregoing observations, we postulate the following mechanism for the epoxidation, metal leaching and H_2O_2 decomposition over M-KIT-6 catalysts (Scheme 1). The tetrahedrally coordinated metal in the KIT-6 matrix forms a metal peroxo complex by reaction with H_2O_2. Experimental evidence for such complex formation on W-grafted MCM-41 material has been previously reported.[29] It is also commonly known that such peroxo species easily undergo reaction with olefinic substrates to form the corresponding epoxide. The peroxo species may either undergo reaction with ethylene leading to the formation of ethylene oxide or undergo solvolysis resulting in the formation of inactive metal oxide species that are easily leached. As shown in Scheme 1, H_2O_2 also undergoes parallel decomposition. Our experimental results indicate that both these deactivation pathways (involving the metal peroxo species and H_2O_2 decomposition) stem from the acidity of M-KIT-6 materials due to metal incorporation. These mechanistic insights therefore suggest that reducing the acidity could minimize, if not eliminate, these adverse side reactions.

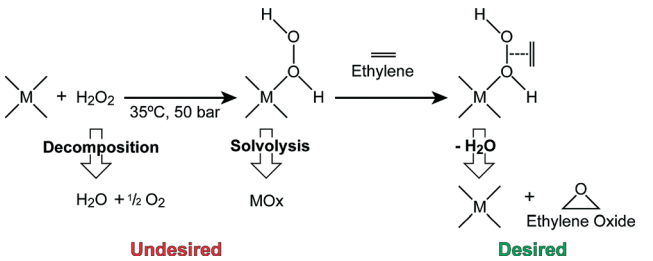

Scheme 1 Proposed reaction/deactivation mechanism. M denotes either W or Nb coordinated tetrahedrally within the KIT-6 matrix.

3.2.3 Performance of silylated catalysts. Silylation, involving the substitution of –OH groups on the catalyst surface by $-OSiR_3$ groups, has been shown to reduce acidity and H_2O_2 decomposition.[30] In addition, silylation is also reported to make the catalyst pores more hydrophobic, thereby excluding water.[31] In an effort to reduce the undesired side reactions, a fresh batch of Nb-KIT-6 (Nb/Si = 40) was silylated according to a reported procedure[32] and tested for ethylene epoxidation. As summarized in Table 2 (entries 20–21), it was found that the silylated catalysts display higher EO selectivity even though the EO yield is lower than that of the calcined catalysts under similar operating conditions. The corresponding H_2O_2 conversion ($X_{H_2O_2}$) in the silylated catalyst was roughly a third of that observed in the calcined catalyst with slightly higher H_2O_2 utilization efficiency ($U_{H_2O_2}$ = 5.3%). It seems plausible that some active metal sites in the catalyst are blocked by long-chain $-OSiR_3$ groups. Further, based on ICP-OES analysis, approximately 25% of the Nb metal leached out of the silylated catalysts after 5 h, which is slightly less than the leaching observed with the calcined but unsilylated catalysts (36% Nb leaching under similar reaction conditions, Table 3, entries 9 and 10). Furthermore, ICP-OES analysis of the spent reaction mixture indicates the leaching of Si (~9%) as well, which was not observed when unsilylated M-KIT-6 catalysts were used. This clearly indicates that the $-OSiR_3$ groups themselves are also being gradually leached. Thus, while silylation techniques partially reduce metal leaching and H_2O_2 decomposition, alternate passivation techniques are required to thwart metal leaching and enhance H_2O_2 utilization. We are currently investigating the use of lower metal loadings (to lower acidity) in conjunction with the use of base pretreatment to reduce the acidity of the catalysts and thereby improve H_2O_2 utilization efficiency.

4. Conclusions

W-KIT-6 and Nb-KIT-6 materials are shown to epoxidize ethylene using H_2O_2 as the oxidant with high EO selectivity under mild reaction conditions (35 °C, 50 bar) where CO_2 formation is avoided. Further, the observed epoxidation activity [30–800 mg EO (g metal)$^{-1}$ h^{-1}] is of the same order of magnitude as that of the conventional Ag-based catalytic process that operates under harsh conditions where substrate/product burning cannot be avoided. Our results suggest that framework-incorporated metal species are significantly more active for epoxidation compared to the extra-framework metal oxide species. Indeed, neat metal oxide species show little, if any, epoxidation activity under similar operating conditions. However, the framework incorporation of the metals introduces Lewis acidity that leads to undesired reactions including solvolysis that result in gradual metal leaching and H_2O_2 decomposition. These mechanistic insights pave the way for developing practically viable epoxidation catalysts in which metal leaching and H_2O_2 decomposition are either minimized or totally avoided.

Acknowledgements

This research was supported partially with funds from the National Science Foundation Accelerating Innovation Research Grant (IIP-1127765).

References

1 M. Ghanta, B. Subramaniam, H. J. Lee and D. H. Busch, *AIChE J.*, 2013, **59**, 180–187.
2 M. O. Ozbek and R. A. van Santen, *Catal. Lett.*, 2013, **143**, 131–141.
3 M. V. Badani, J. R. Monnier and M. A. Vannice, *J. Catal.*, 2002, **206**, 29–39.
4 J. C. Dellamorte, J. Lauterbach and M. A. Barteau, *Ind. Eng. Chem. Res.*, 2009, **48**, 5943–5953.
5 M. Ghanta, *Doctoral dissertation*, University of Kansas, 2012.
6 B. Subramaniam, D. H. Busch, H. J. Lee, M. Ghanta and T-P. Shi, Process for selective oxidation of olefins to epoxides, *US Pat.* 8,080,677 B2, Issued Dec 20, 2011.
7 M. Ghanta, T. Ruddy, D. Fahey, D. Busch and B. Subramaniam, *Ind. Eng. Chem. Res.*, 2013, **52**, 18–29.
8 B. Subramaniam and G. R. Akien, *Curr. Opin. Chem. Eng.*, 2012, **1**, 336–341.
9 D. Hoegaerts, B. F. Sels, D. E. de Vos, F. Verpoort and P. A. Jacobs, *Catal. Today*, 2000, **60**, 209–218.
10 I. Nowak, B. Kilos, M. Ziolek and A. Lewandowska, *Catal. Today*, 2003, **78**, 487–498.
11 H. Y. Wu, X. L. Zhang, C. Y. Yang, X. Chen and X. C. Zheng, *Appl. Surf. Sci.*, 2013, **270**, 590–595.
12 J. M. R. Gallo, I. S. Paulino and U. Schuchardt, *Appl. Catal., A*, 2004, **266**, 223–227.
13 M. Selvaraj, S. Kawi, D. W. Park and C. S. Ha, *J. Phys. Chem. C*, 2009, **113**, 7743–7749.
14 J. Y. Tang, L. Wang, G. Liu, Y. Liu, Y. Z. Hou, W. X. Zhang, M. J. Jia and W. R. Thiel, *J. Mol. Catal. A: Chem.*, 2009, **313**, 31–37.
15 C. Tiozzo, C. Bisio, F. Carniato, L. Marchese, A. Gallo, N. Ravasio, R. Psaro and M. Guidotti, *Eur. J. Lipid Sci. Technol.*, 2013, **115**, 86–93.
16 E. Poli, J. M. Clacens, J. Barrault and Y. Pouilloux, *Catal. Today*, 2009, **140**, 19–22.
17 A. Ramanathan, B. Subramaniam, D. Badloe, U. Hanefeld and R. Maheswari, *J. Porous Mater.*, 2012, **19**, 961–968.
18 A. Ramanathan, R. Maheswari, D. H. Barich and B. Subramaniam, *Microporous Mesoporous Mater.*, 2014, **190**, 240–247.
19 B. Subramaniam, A. Ramanathan, M. Ghanta and W. Yan, *Alkylene epoxidation with mesoporous catalysts*, WO2014004768 A2, Published Jan 3, 2014.
20 T. W. Kim, F. Kleitz, B. Paul and R. Ryoo, *J. Am. Chem. Soc.*, 2005, **127**, 7601–7610.
21 F. Kleitz, D. Liu, G. M. Anilkumar, I.-S. Park, L. A. Solovyov, A. N. Shmakov and R. Ryoo, *J. Phys. Chem. B*, 2003, **107**, 14296–14300.

22 J. E. Buffum, R. M. Kowaleski and W. H. Gerdes, Ethylene oxide catalyst, *US Pat.* 5145824 A, Issued Sep 8, 1992.
23 H. S. Fogler, *Elements of chemical reaction engineering*, Prentice-Hall, 1992.
24 A. Ramanathan, B. Subramaniam, R. Maheswari and U. Hanefeld, *Microporous Mesoporous Mater.*, 2013, **167**, 207–212.
25 B. Kilos, M. Aouine, I. Nowak, M. Ziolek and J. C. Volta, *J. Catal.*, 2004, **224**, 314–325.
26 R. A. Sheldon, M. Wallau, I. W. C. E. Arends and U. Schuchardt, *Acc. Chem. Res.*, 1998, **31**, 485–493.
27 M. C. Capel-Sanchez, J. M. Campos-Martin and J. L. G. Fierro, *Appl. Catal., A*, 2003, **246**, 69–77.
28 L. J. Davies, P. McMorna, D. Bethell, P. C. B. Page, F. King, F. E. Hancock and G. J. Hutchings, *J. Mol. Catal. A: Chem.*, 2001, **165**, 243–247.
29 M. Morey, J. Bryan, S. Schwarz and G. Stucky, *Chem. Mater.*, 2000, **12**, 3435–3444.
30 M. Ramakrishna Prasad, M. S. Hamdy, G. Mul, E. Bouwman and E. Drent, *J. Catal.*, 2008, **260**, 288–294.
31 M. V. Cagnoli, S. G. Casuscelli, A. M. Alvarez, J. F. Bengoa, N. G. Gallegos, M. E. Crivello, E. R. Herrero and S. G. Marchetti, *Sel. Contrib. XIX Ibero Am. Catal. Symp.*, 2005, vol. 107–108, pp. 397–403.
32 J. M. R. Gallo, H. O. Pastore and U. Schuchardt, *J. Catal.*, 2006, **243**, 57–63.